



## OPEN

SUBJECT AREAS:  
CANCER PREVENTION  
ONCOGENESISReceived  
5 November 2013Accepted  
24 March 2014Published  
10 April 2014Correspondence and  
requests for materials  
should be addressed to  
M.Y.L. (Limingyi63@  
yahoo.cn) or R.Z.Z.  
(hepatolab@gmail.  
com)

# Dihydromyricetin promotes hepatocellular carcinoma regression via a p53 activation-dependent mechanism

Qingyu Zhang<sup>1</sup>, Jie Liu<sup>1</sup>, Bin Liu<sup>1</sup>, Juan Xia<sup>1</sup>, Nianping Chen<sup>1</sup>, Xiaofeng Chen<sup>1</sup>, Yi Cao<sup>2</sup>, Chen Zhang<sup>2</sup>, Caijie Lu<sup>1</sup>, Mingyi Li<sup>1</sup> & Runzhi Zhu<sup>1</sup><sup>1</sup>Key Laboratory of Hepatic Disease, Department of Hepatobiliary Surgery, Affiliated Hospital of Guangdong Medical College, Zhanjiang 524001, China, <sup>2</sup>Laboratory of Molecular and Experimental Pathology, Key Laboratory of Animal Models and Human Disease Mechanisms of CAS and Yunnan Province, Kunming Institute of Zoology, Chinese Academy of Sciences, Kunming, People's Republic of China, Kunming 650223, China.

The development of antitumor chemotherapy drugs remains a key goal for oncologists, and natural products provide a vast resource for anti-cancer drug discovery. In the current study, we found that the flavonoid dihydromyricetin (DHM) exhibited antitumor activity against liver cancer cells, including primary cells obtained from hepatocellular carcinoma (HCC) patients. In contrast, DHM was not cytotoxic to immortalized normal liver cells. Furthermore, DHM treatment resulted in the growth inhibition and remission of xenotransplanted tumors in nude mice. Our results further demonstrated that this antitumor activity was caused by the activation of the p53-dependent apoptosis pathway via p53 phosphorylation at serine (15Ser). Moreover, our results showed that DHM plays a dual role in the induction of cell death when administered in combination with cisplatin, a common clinical drug that kills primary hepatoma cells but not normal liver cells.

Liver cancer is a major malignant tumor worldwide and is the third most common cause of cancer-related mortality<sup>1</sup>. Over 80% of liver cancer patients are diagnosed with hepatocellular carcinoma (HCC), which is resistant to most conventional chemotherapeutic agents<sup>2</sup>. Moreover, the use of chemoprevention agents is typically associated with side effects that lead to the destruction of normal tissues, such as those of the digestive, hematopoietic and nervous systems<sup>3–5</sup>. The development of drugs that specifically target tumor cells, but not normal cells, represents a common goal in drug development.

Traditional Chinese medicine is grounded in several thousand years of clinical application experience<sup>6</sup>, and essential components of Chinese medicine have been used to treat cancer. For example, Chinese scientists have demonstrated that the Chinese medicine arsenic trioxide (As<sub>2</sub>O<sub>3</sub>), which is used in the management of syphilis and psoriasis, is also therapeutically effective in patients with acute promyelocytic leukemia (APL)<sup>7</sup>. Natural compounds contain various types of medicinal ingredients, including vitamin derivatives, phenolic and flavonoid agents, organic sulfur compounds, isothiocyanates, curcumins, fatty acids and d-limonene<sup>8–10</sup>, and sufficient evidence has demonstrated that these components can substantially inhibit tumor formation<sup>8</sup>.

Dihydromyricetin (DHM), a flavonoid component isolated from *hovenia dulcis*, functions as an anti-intoxicant, anti-inflammatory and anti-oxidative agent<sup>11,12</sup>. Recent studies have further suggested that DHM acts as an anti-tumor agent<sup>13,14</sup>, although it remains unknown whether this drug displays efficacy in hepatic cancer. Therefore, the current study sought to evaluate whether DHM promotes liver tumor regression and to identify the mechanisms involved.

## Results

**DHM specifically induces apoptosis in HCC cells but has little effect on normal immortalized liver cells.** We used HepG2 cells and three primary cell lines that had been freshly isolated from lesion loci of HCC patients. These cells were seeded at a density of  $3 \times 10^5$  cells/cm<sup>2</sup> 12 h prior to DHM treatment. The cells were exposed to various DHM concentrations (0, 10, 25, 50, 75, 100, 150 and 200  $\mu$ M), and DMSO served as the drug vehicle. The data indicated that DHM induced growth repression and apoptosis in HepG2 cells in a dose- and time-dependent manner (Fig. 1 A). Apoptosis was also induced in primary cultured 4401 liver cancer cells after DHM exposure



(Fig. 1 B). Next, we evaluated whether DHM was cytotoxic to normal liver cells. Interestingly, DHM did not induce cell death in the immortalized normal human liver cell line HL7702 (Fig. 1 B). We then compared the cell death ratio of three cell lines exposed to various DHM concentrations using a viable cell counting assay (Fig. 1 C), and we used an Annexin V apoptosis assay kit (BD, USA) to detect cell apoptosis by flow cytometry. These results confirmed that DHM selectively targeted liver cancer cells and promoted cancer cell apoptosis. In fact, DHM improved survival in HL7702 cells rather than inducing cell death (Fig. 1 D&E). Moreover, DHM inhibited proliferation in HepG2 cells (Fig. 1 F&G) but demonstrated weak proliferative inhibition in L02 and HL7702 immortalized normal liver cells (Fig. 1 F&G). We next analyzed the half-maximal inhibitory concentration ( $IC_{50}$ ) of DHM in HepG2, HL7702 and L02 cells using the MTT assay. The  $IC_{50}$  values at 12, 24 and 48 h were 140, 127 and 55  $\mu$ M, respectively, in HepG2 cells (Fig. 1 H). Of note, DHM demonstrated no significant effects on HL7702 and L02 cell viability (Fig. 1 I&J).

**DHM regulates survival signals and activates the apoptosis-related signaling pathway.** Upon further investigation, we observed an accumulation of apoptosis-related proteins following DHM stimulation. In particular, the apoptosis-related caspase 3 and caspase 8 proteins were downregulated following DHM treatment, whereas the expression of caspase 9 was not altered. Moreover, the activated forms of caspases, such as cleaved caspase 8 and cleaved caspase 3, were present in increased amounts following DHM treatment (Fig. 2 A&C), and apoptosis-related Bcl-2 protein family members, including BAX, BAK and BAD, were also activated. In addition, PARP function (related to DNA repair) was lost via enhanced splicing, which led to cancer cell apoptosis (Fig. 2A). Of note, DHM treatment did not affect the caspase and Bcl-2 family members in the normal liver cell line HL7702 (Fig. 2 B). AKT, also known as protein kinase B (PKB), is a serine/threonine-specific protein kinase that plays a key role in cell apoptosis, proliferation and migration<sup>15</sup>. AKT is an anti-apoptotic factor under conditions of cell stress<sup>16</sup>, and our results indicated that DHM treatment decreased total AKT protein levels and thus reduced AKT phosphorylation (serine (Ser)473) in HepG2 and SMMC-7721 cells but showed no effect in HL7702 cells (Fig. 2 D–G).

**DHM induces apoptosis by enhancing TP53 expression and phosphorylation at Ser15.** DHM increased total p53 and downstream p21 expression after 12 h of treatment (Fig. 3 A&B). Interestingly, we observed increased p53 phosphorylation (p-p53) at serine 15 and 20. In particular, p53 that was phosphorylated at Ser15 upon DHM treatment was translocated from the cytoplasm to the nuclear region. Using immunofluorescence (IF) microscopy, we detected nuclear accumulation of p53 phosphorylated at Ser15 (Fig. 3 A). Phosphorylation of p53 at Ser15 and Ser20 is known to inhibit its interaction with MDM2 protein, a negative regulator of p53. We found that p53 phosphorylation at Ser15 was upregulated and that MDM2 mRNA levels were negatively correlated with p53 mRNA levels (Fig. 3 C&D). We validated these results using q-RT PCR for p53 target genes (*p21* and *Bak*) to confirm the hypothesis that DHM induced the expression of apoptosis- and anti-proliferation-related genes regulated by p53 (Fig. 3 E&F).

**p53 inhibition rescues DHM-mediated cell death.** Pifithrin- $\alpha$  (PFT $\alpha$ ), a small molecule p53 inhibitor, inhibits gene expression by preventing p53 translocation from the cytoplasm to the nucleus. Our results indicated that PFT $\alpha$  rescued DHM-induced cell death in HepG2 cells (Fig. 4 A–C). Furthermore, we found that PFT $\alpha$  completely reversed DHM-mediated p53 phosphorylation at Ser15 and the nuclear accumulation of this protein (Fig. 4 D). The expression of p53 and its downstream proteins was also reversed by PFT $\alpha$  (Fig. 4 E), thereby implicating p53 in DHM-induced cell

death. Next, to evaluate the mechanism responsible for the increased expression of p53, we assessed MDM2, a negative regulator of p53 that plays a key role in p53 degradation. We found that the MDM2 protein levels were decreased upon treatment with DHM and that this effect was inhibited by PFT $\alpha$  treatment. p21 is a target protein that regulates the activation of p53-regulated genes. Our results demonstrated that p21 expression was elevated following DHM treatment, whereas this effect was reversed by PFT $\alpha$  (Fig. 4 E). To confirm this observation, we used siRNA to specifically block endogenous p53 expression in SMMC-7721 cells (Fig. 4 F). After p53 expression was reduced in SMMC-7721 cells, cell apoptosis was not observed following DHM treatment (Fig. 4 G&H). These experiments strongly demonstrate that DHM-induced liver cancer cell apoptosis is p53 dependent.

**DHM inhibits tumor growth in vivo.** To investigate the effects of DHM on tumor growth *in vivo*, we used a mouse xenograft tumor model. DHM treatment for 21 days did not significantly impact body weight (Fig. 5 A), although the tumor volume was significantly inhibited ( $43.5 \pm 20\%$  inhibition at 500 mg/kg DHM compared to the CMC-Na control group) (Fig. 5 B&C). Moreover, the levels of total and phosphorylated p53 in the tumors were increased in the DHM-treated group compared to the CMC-Na control group (Fig. 5 D&E). These results indicate that DHM inhibits tumor growth *in vivo*, possibly through the upregulation of p53 and p-p53 (Ser15).

**DHM and cisplatin cooperate to relieve cisplatin cytotoxicity in HL7702 normal liver cells but not in primary hepatoma cells.** The side effects of chemotherapeutics in normal tissues represent a major obstacle for anticancer drug development<sup>5</sup>. An ideal anticancer drug represses tumor cell growth with minimal side effects in normal tissues. We observed that cisplatin, a classic clinical drug for cancer management, caused damage to HL7702 normal liver cells. However, we found that DHM prevented cisplatin-induced cell apoptosis in HL7702 cells (Fig. 6 A&B). Interestingly, protection by DHM was not observed in primary cells isolated and cultured from hepatoma patients (Fig. 6 E&F). We next sought to evaluate the role of p53 in this process, and our results indicated that p53 was not induced in HL7702 cells but was elevated in 4401 primary hepatoma cells. Moreover, the cisplatin-induced p53 upregulation was reversed by DHM in HL7702 cells, whereas no effect was observed in 4401, 1204 or 4404 cells (Fig. 6 C–E). Thus, we concluded that DHM-regulated p53 accumulation plays an important role in alleviating cisplatin-mediated normal cell death.

## Discussion

Natural products have been widely used in the development of anticancer drugs, although the mechanism of cancer cell suppression remains difficult to explain. Nevertheless, Chinese medicine has been practiced for thousands of years, and historical experience demonstrates the definitive effect of Chinese medicine in the treatment of disease<sup>17–19</sup>. DHM is the primary medicinal flavonoid extracted from *Ampelopsis grossedentata*. In the current study, we explored the anti-neoplastic effects of DHM in liver tumorigenesis, and we found that DHM displayed antitumor activity in several hepatoma cell lines, including HepG2 and SMMC-7721. Furthermore, DHM also demonstrated anticancer activities in cultured cells obtained from three HCC patients. However, it is important to note that DHM did show equivalent effects in all liver tumor cells examined, as MHCC97L, SK-Hep-1, QGY7703 were insensitive to DHM treatment (data not shown). In addition, we tested the acute toxicity of DHM at concentrations ranging from 150 mg/kg (500  $\mu$ mol/L) to 1.5 g/kg (5,000  $\mu$ mol/L) body weight in mice; we observed no significant side effects to mice. Because body fluid only accounts for 60% of body weight and taking bioavailability into account, we estimated that 100  $\mu$ mol/L DHM is a safe concentration. Second, we

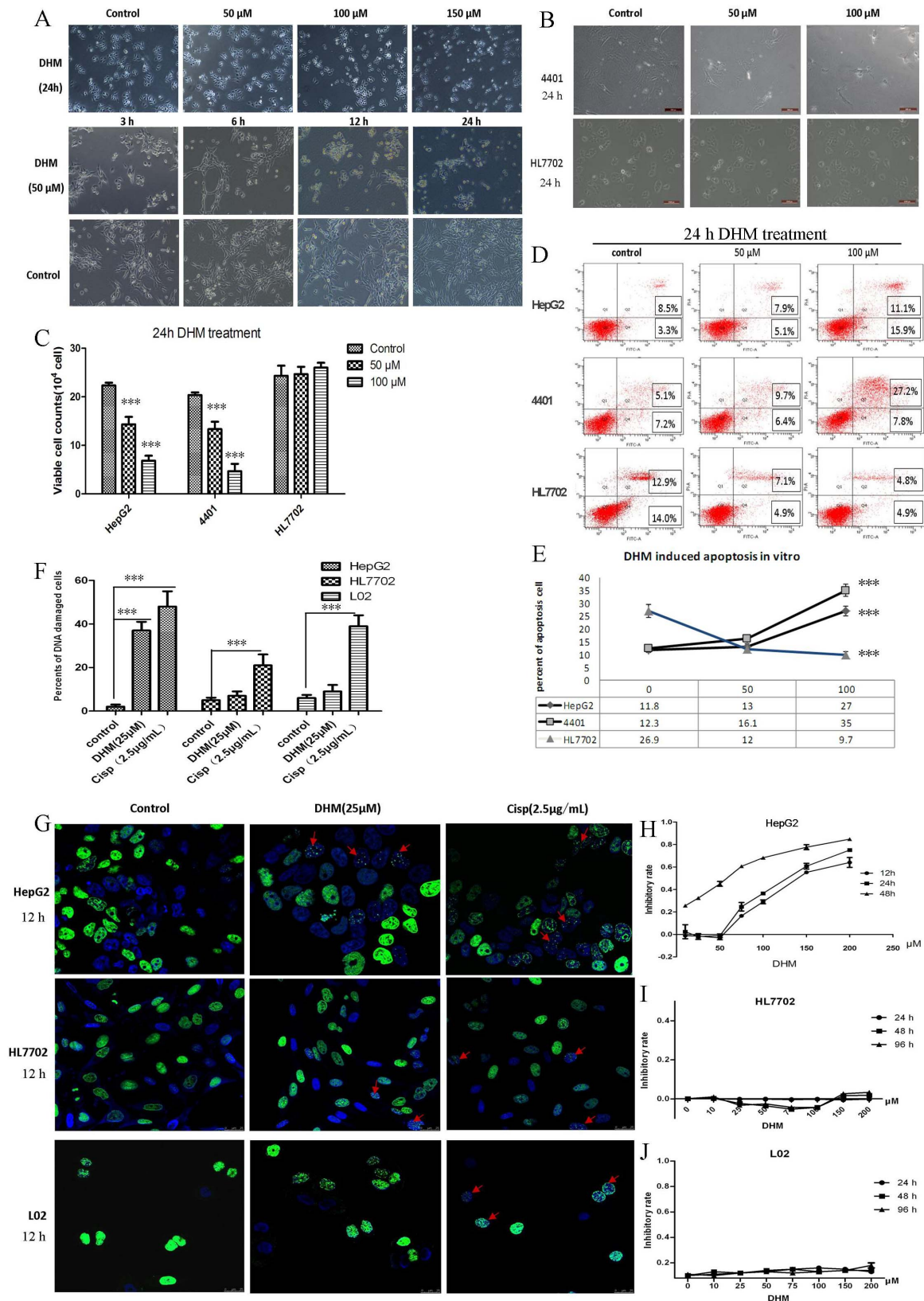


**Figure 1** | DHM specifically induces apoptosis in HCC cells but has little effect on normal immortalized liver cells. (A) DHM induced apoptosis in HepG2 cells in a time- and concentration-dependent manner. (200× magnification) (B) Cell growth was inhibited in 4401 primary cells and HL7702 cells after 24 h of exposure to DHM at various concentrations (200× magnification). (C) The viable cell count of HepG2, HL7702 and 4401 primary cells after treatment with DHM ( $n = 6$ , Mean  $\pm$  SD). (D, E) DHM-induced apoptosis in HepG2, HL7702 and 4401 cells was detected by flow cytometry (Mean  $\pm$  SD, 24 h treatment). (F, G) DHM or cisplatin inhibited the proliferation of HepG2, HL7702 and L02 cells, as assessed by the Edu incorporation assay (Mean  $\pm$  SD, DHM: 25  $\mu$ M, cisplatin: 2.5  $\mu$ g/mL, 12 h treatment). (H–J) The DHM inhibitory rate in HepG2, HL7702 and L02 cells was assessed by MTT assay (Mean  $\pm$  SD).

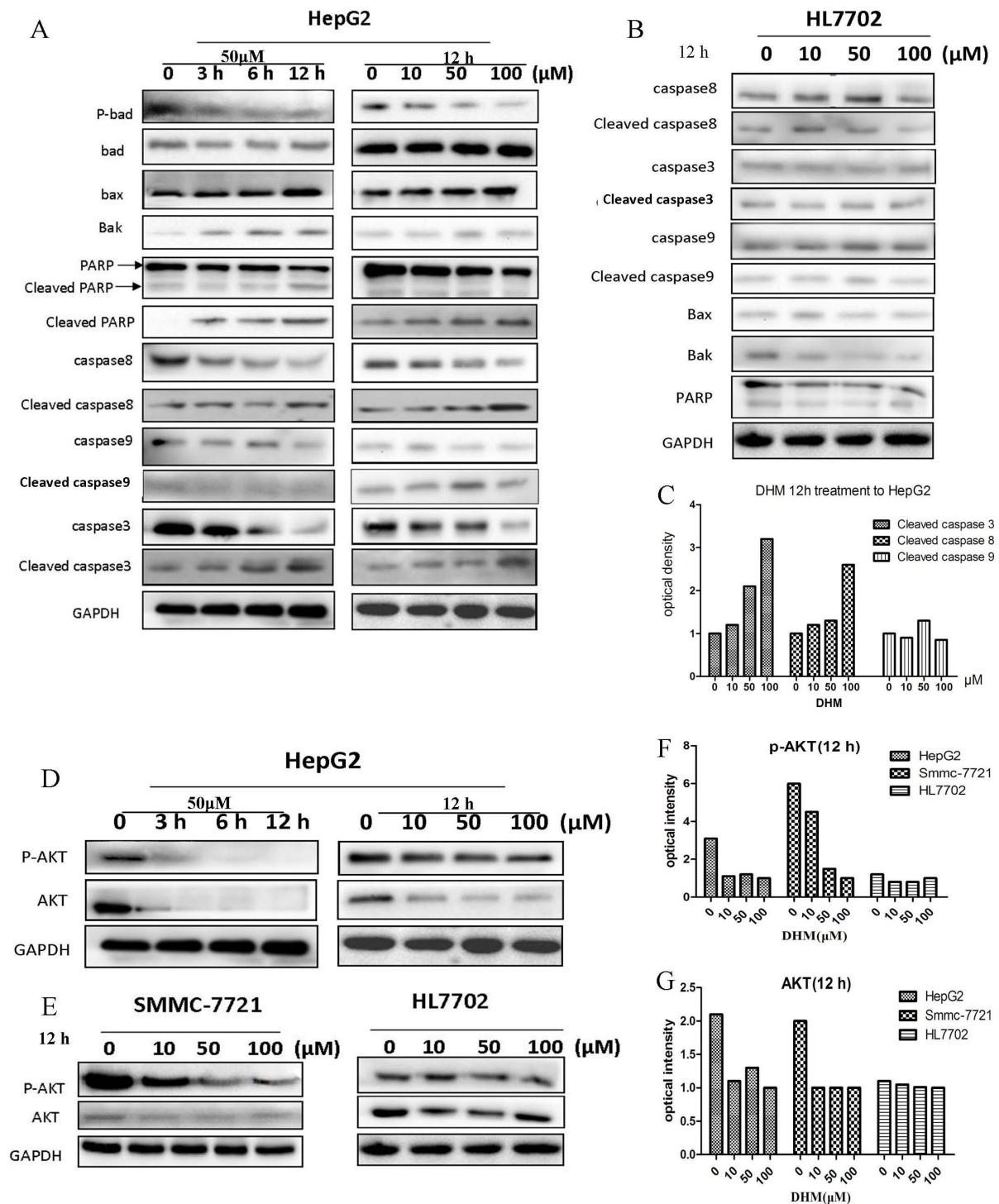


**Figure 2** | DHM regulates survival signals and activates the apoptosis-related signaling pathway. (A) The expression of apoptosis-related proteins in HepG2 cells after DHM treatment. (B) The expression of apoptosis-related proteins in HL7702 cells after DHM treatment (12 h DHM treatment). (C) Activated caspase proteins (cleaved caspases) were quantified by optical density analysis. (D) AKT and p-AKT proteins were reduced in HepG2 cells after DHM stimulation (12 h treatment). (E) AKT and p-AKT proteins were downregulated in SMMC-7721 but not affected in HL7702 cells after DHM stimulation. (F, G) p-AKT and AKT proteins were quantified by optical analysis in HepG2, SMMC-7721 and HL7702 cells.

have demonstrated that DHM inhibits liver cancer cell (HepG2) proliferation and induces apoptosis at concentrations of 10–150  $\mu$ mol/L<sup>14</sup>. These results indicate that DHM is a potentially non-cytotoxic compound that regulates various target genes implicated in tumor cell proliferation and apoptosis.

AKT is a key protein that mediates cell survival, and it is therefore a potential target for cancer management<sup>20,21</sup>. In our study, DHM

inhibited HepG2 cell proliferation *in vitro* and resulted in the reduced expression of AKT and p-AKT protein. Of note, this phenomenon was also observed in other liver cancer cell lines. Previous studies have demonstrated that AKT inhibits BAD via direct phosphorylation, thereby preventing Bim expression by phosphorylating and inhibiting the Forkhead family of transcription factors (FoxO)<sup>22</sup>. Furthermore, AKT was shown to phosphorylate BAD at Ser136,

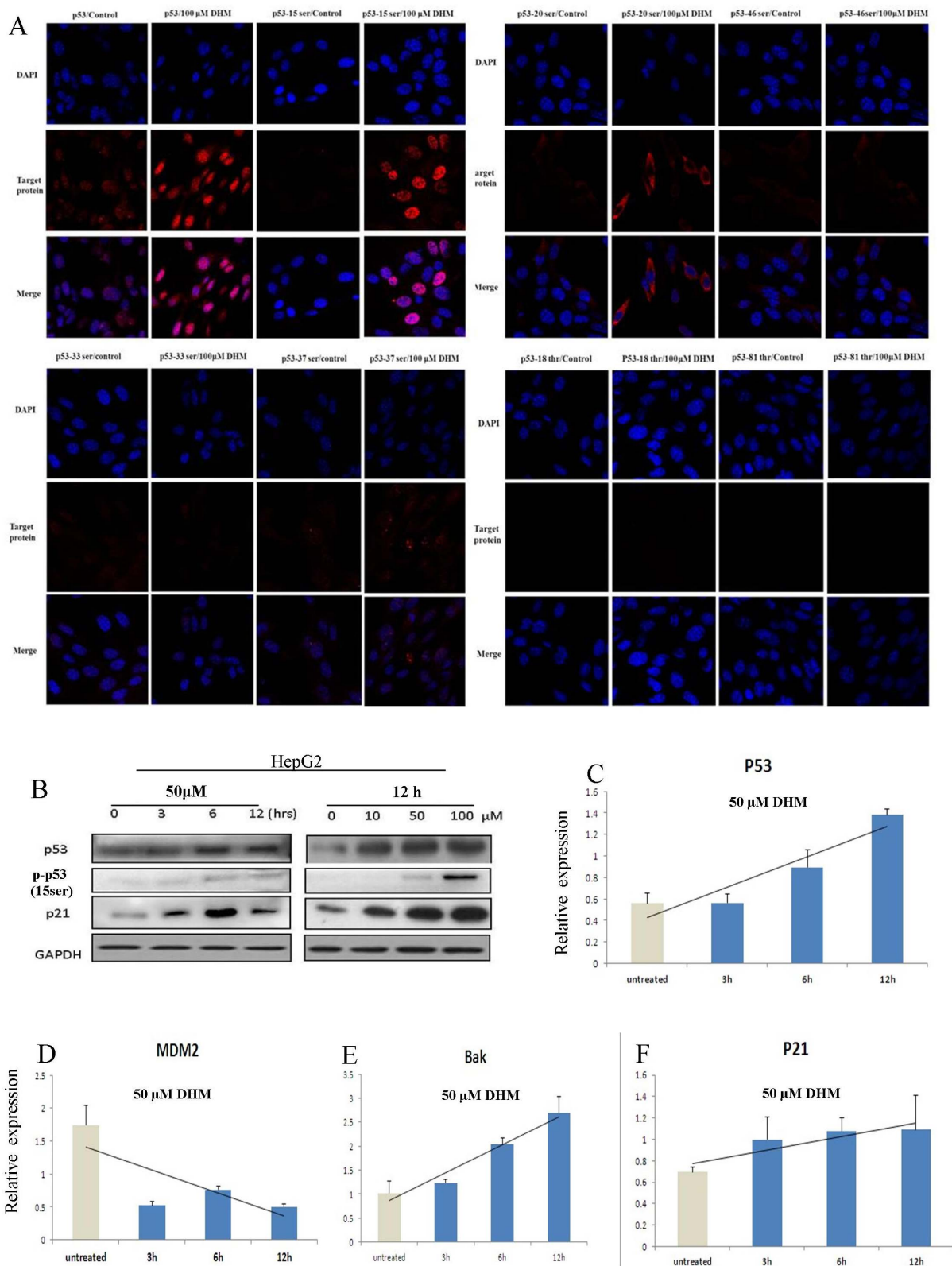
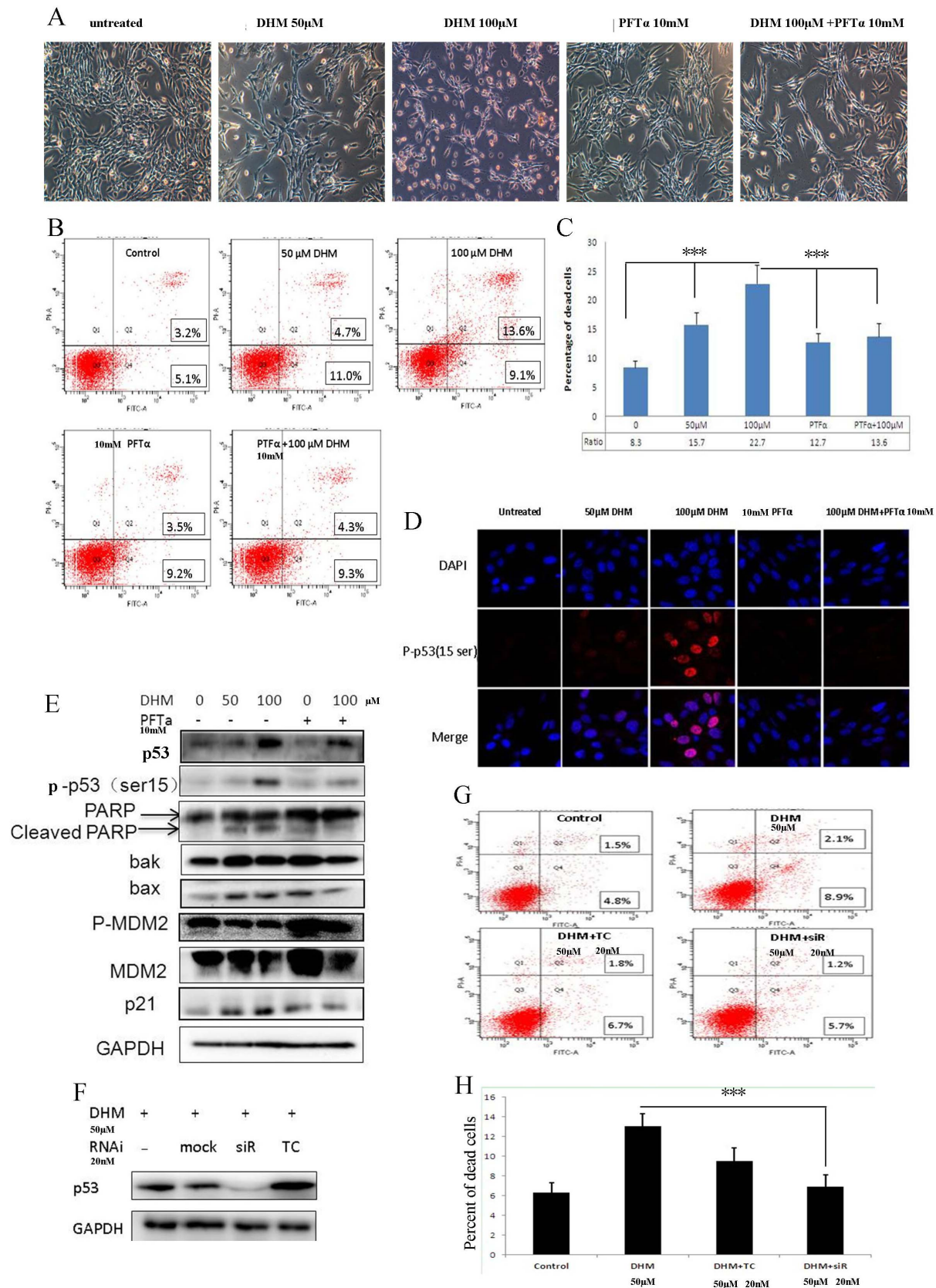


**Figure 3 | DHM induces apoptosis by enhancing TP53 expression and phosphorylation at Ser15. (A)** Various p53 phosphorylation sites were determined by IF (12 h DHM treatment). **(B)** DHM affected p53, p-p53 and p21 protein levels (western blot). **(C, D, E, F)** The mRNA levels of p53, p21, MDM2 and Bak at various time points following DHM exposure were analyzed by q-PCR (Mean  $\pm$  SD).

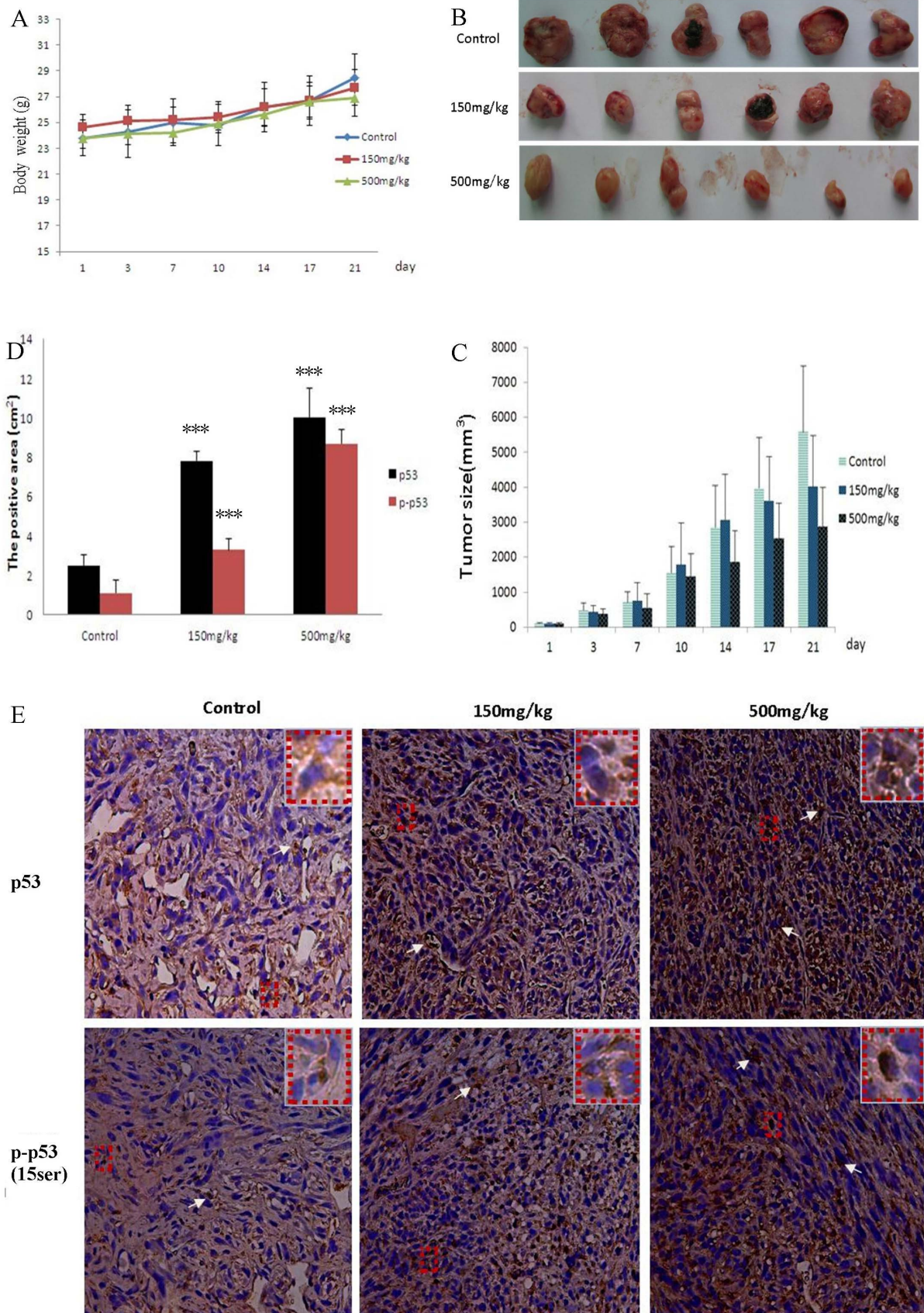
thereby causing BAD to dissociate from the Bcl-2/Bcl-XL complex and lose its pro-apoptotic function<sup>22</sup>. We observed that DHM decreased Bad phosphorylation, which is consistent with AKT downregulation after DHM stimulation. In addition, we found that

AKT was not significantly altered in HL7702 cells, suggesting that DHM displays no side effects in healthy cells.

Cell death is associated with caspase activation and apoptosis-related protein (Bcl-2 family) accumulation. In this study, we



**Figure 4** | p53 inhibition rescues DHM-mediated cell death. (A) PFT $\alpha$  (10 mM) reversed DHM-induced cell apoptosis. (200 $\times$  magnification). (B, C) Annexin V/PI was used to detect apoptosis after PFT $\alpha$  administration (Mean  $\pm$  SD, 24 h DHM treatment). (D) p53 phosphorylation at serine 15 was measured by IF after PFT $\alpha$  treatment. (E) The expression of p53 and apoptosis-related proteins was detected after PFT $\alpha$  treatment by western blot. (F) SMMC-7721 cells were transfected with p53 siRNA to block the DHM-induced p53 upregulation. (G, H) The cell death percentage was determined by flow cytometry in SMMC-7721 cells with or without p53 siRNA transfection after DHM treatment (Mean  $\pm$  SD, 24 h DHM treatment after siRNA (20 nM) transfection).



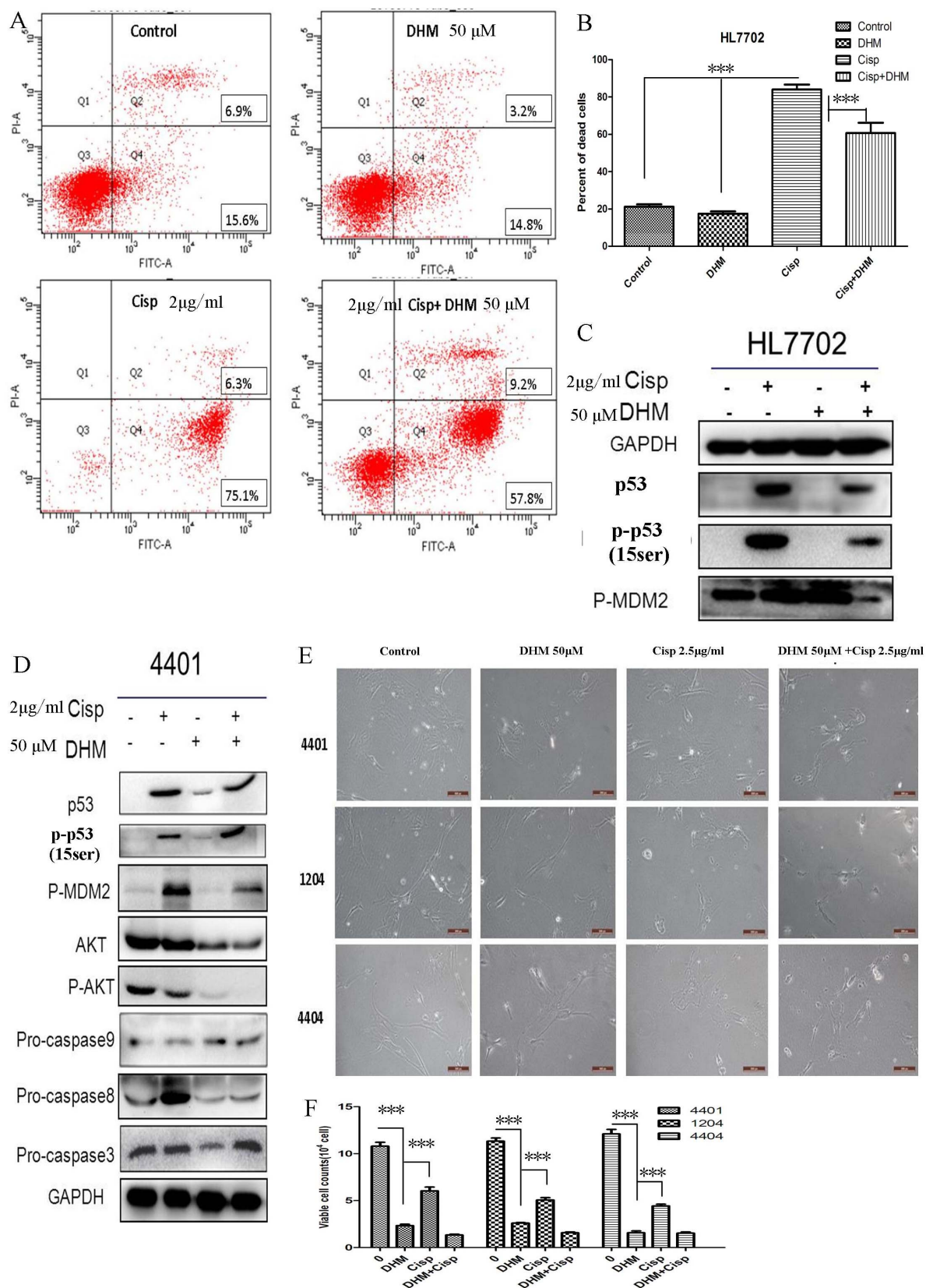


**Figure 6 | DHM and cisplatin cooperate to relieve cisplatin cytotoxicity in HL7702 normal liver cells but not in primary hepatoma cells.** (A, B) Cell death was analyzed by flow cytometry (Mean  $\pm$  SD, 24 h treatment, 50  $\mu$ M DHM, 2  $\mu$ g/ml cisplatin). (C, D) The expression of p53, p-p53 (15ser), AKT, p-AKT, p-MDM2 and caspase family proteins was evaluated by western blot in HL7702 and 4401 cells (24 h treatment, 50  $\mu$ M DHM, 2  $\mu$ g/ml cisplatin). (E) Primary HCC cell death was measured under a phase contrast microscope at 200 $\times$  magnification (24 h treatment, 50  $\mu$ M DHM, 2  $\mu$ g/ml cisplatin). (F) The viable cells were counted and analyzed after drug treatment (n = 6, Mean  $\pm$  SD, 24 h treatment, 50  $\mu$ M DHM, 2  $\mu$ g/ml cisplatin).



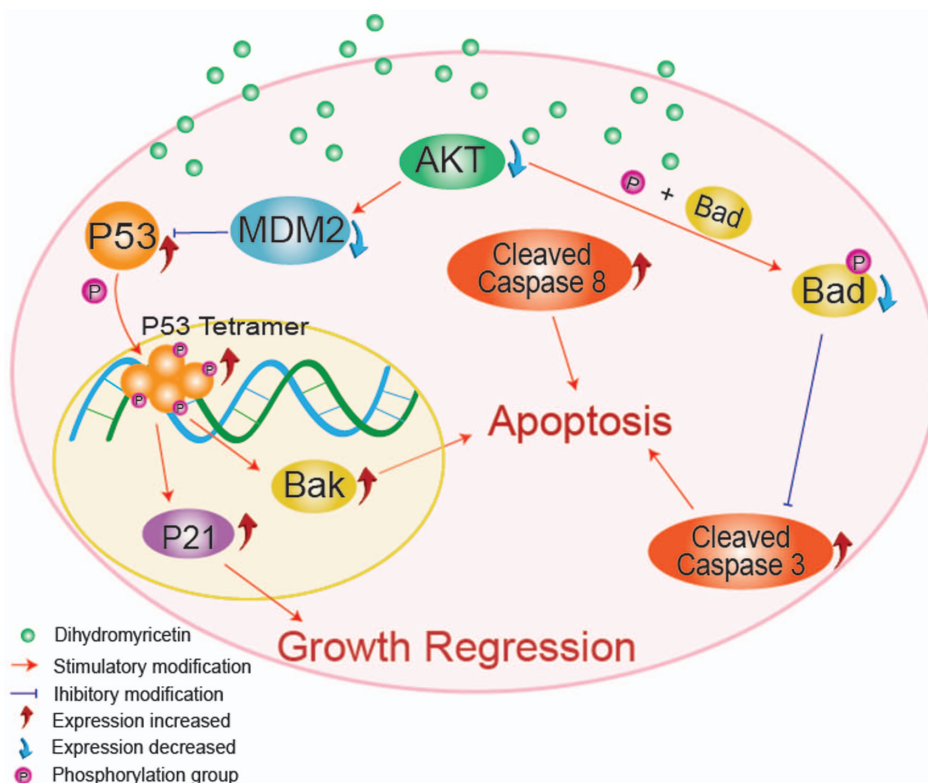


**Figure 7 | The molecular mechanism of DHM-induced liver cancer cell growth regression and apoptosis.** The AKT pathway was inhibited by DHM treatment, and Bad phosphorylation was reduced, which resulted in tumor cell apoptosis. In addition, tumor cell growth regression and apoptosis resulted from the transcriptional activation of the *P21* and *BAK* genes in a p53-dependent manner.

evaluated the major caspases, including caspases 9, 8 and 3, and their respective activated forms (cleaved caspases 9, 8 and 3). In addition, Bcl-2 family proteins were also assessed. Our results indicated that apoptosis was induced in HepG2 cells after exposure to DHM. We also tested the normal liver cell line HL7702, although no apoptosis-related protein alterations were observed. These results demonstrated that DHM selectively induced apoptosis in liver cancer cells but not normal cells.

p53 is a tumor suppressor that acts as a genomic stability guardian and apoptosis executioner after cellular exposure to a variety of stresses<sup>23,24</sup>. Initially, we sought to address whether p53 was responsive to DHM stimulation and, if p53 was upregulated by DHM, whether cell apoptosis would be induced in the tumor. p53 is known as the master guardian and executioner of cell apoptosis, and p53 upregulation correlates with *TP53* gene expression and degradation ratio. Moreover, p53 proteins determine the fate of cancer cells, and p53 protein stabilization is related to its modification status and its negative regulation by the activities of proteins such as MDM2<sup>25,26</sup>. MDM2, a p53-specific E3 ubiquitin ligase, plays a pivotal role in limiting p53 cellular accumulation. In particular, phosphorylation at Ser15 impairs MDM2 binding to p53, promoting both the accumulation and activation of p53 in response to DNA damage<sup>27</sup>. Our results suggest that DHM increases intracellular p53 protein levels, particularly the phosphorylation of p53 at Ser15. This result indicates that DHM potentially induces cell apoptosis through activation of the p53 pathway via increased p53 phosphorylation at Ser15, thereby inhibiting p53 degradation by MDM2, a negative regulator of p53. Moreover, p53 inhibitors and siRNA were used to block p53, and we found that DHM-induced cell death could be reversed. Furthermore, DHM inhibited the growth of xenograft tumors in nude mice, and immunohistochemistry (IHC) performed on tumor tissue samples indicated that the p53 and p-p53 (15Ser) levels were increased in the DHM-treated group, confirming our hypothesis *in vivo*. Together,

these results demonstrate that DHM induces apoptosis in liver cancer cells by increasing the level of p53 and promoting p53 phosphorylation at Ser15 (Fig. 7).

Finally, we evaluated whether DHM is both cytotoxic to liver cancer and relieves the side effects of the chemotherapy agents that are typically used to treat human HCC patients. Therefore, we treated primary cells obtained from HCC patients and HL7702 normal liver cells with DHM and cisplatin in combination. Interestingly, we found that DHM did not significantly enhance the inhibitory effects of cisplatin in primary liver cancer cells; however, DHM alleviated cisplatin-mediated damage to HL7702 cells. Furthermore, western blot results indicated that p53 was upregulated after cisplatin treatment in primary cancer cells and HL7702 cells. DHM also increased p53 expression in primary cancer cells but displayed no effect on p53 expression in HL7702 cells. The difference between the DHM response of malignant and non-malignant cells may result from the change of p-MDM2. Our result showed that p-MDM2 level was increased significantly in 4401 cells compared with HL7702 cells after DHM treatment (Fig. 6). The upregulation of p-MDM2 resulted in p53 degradation in HL7702 cells. In contrast, p53 accumulated in 4401 cells because of non-change of p-MDM2 after DHM exposure. In fact, it is important to note that DHM downregulated p53 expression in HL7702 cells, whereas p53 expression was not altered in primary cancer cells when cooperated with cisplatin administration. Thus, we speculate that DHM not only induces apoptosis in hepatoma cells but also protects normal liver cells after chemotherapeutic exposure. DHM may serve as a potential chemotherapeutic compound for HCC management.

## Methods

**Cell culture and drug treatment.** The human hepatic cancer cell lines HepG2 and SMMC-7721 as well as the immortalized liver cell lines HL7702 and L02 were used in this study. The HepG2 and SMMC-7721 cell lines were kindly provided by Dr. Yan Yu (Shanghai Jiao Tong University, Shanghai, China). The HL7702 cell line was



obtained from Dr. Yi Cao (Molecular Pathology Laboratory, Kunming Institution of Zoology, Chinese Academy of Science, Kunming, China). The L02 cell line was purchased from CellBank of Shanghai. All of the cell lines were cultured in RPMI1640 medium supplemented with 10% fetal bovine serum and 2 mM L-glutamine. DHM (Cat: SML0295) was purchased from Sigma. DHM powder was dissolved in DMSO to create a stock at a concentration of 50  $\mu$ M, which was subsequently diluted in culture medium to the desired concentration for experiments. DMSO was used as the vehicle control.

**Primary cell cultures.** Patient biopsies were diagnosed by a pathologist, and HCC specimens removed from these patients were immediately dissociated using surgical scissors. The samples were treated with 0.5% trypsin for primary cell isolation and cultured in DMEM/F12 medium containing 20% fetal bovine serum. We established three stable primary cell lines: 4401, 4403 and 1204. The primary cells used in our study were cultured for 10 or fewer passages.

**Cell proliferation assay.** The Click-iT<sup>®</sup> EdU cell proliferation assay kit (cat: C10337, Lifetechnologies, USA) was used to assess cell proliferation via the detection of new DNA synthesis. Cells were cultured in a glass dish (Nest, China) until they were 50% confluent. The cells were then treated with DHM (25  $\mu$ M) or cisplatin (positive control, 2.5  $\mu$ g/ml). After 12 h of treatment, the medium was removed, and the cells were washed with PBS. Serum-free medium supplemented with 10  $\mu$ M EdU was used to detect new DNA synthesis. After 10 h, the cells were washed with PBS, fixed (3.7% formaldehyde) and permeabilized (0.05% triton X-100 in PBS). Edu incorporation was detected using the Click-iT<sup>®</sup> reaction cocktail. Image capture was performed using TCP-SP5 laser confocal microscope (Leica, Germany). The images were processed using the Image J software.

**MTT assay.** Cells were seeded in 96-well plates at a density of 5,000 cells per well. After 12 h, DHM (four replicates in each group) was added at varying concentrations for various durations. Then, 10  $\mu$ L MTT solution (5 mg/ml) was added to each well, and the plates were incubated for 2 h at 37°C. The medium was removed, and 150  $\mu$ L DMSO was added to completely dissolve the formazan crystals. The absorbance at 570 nm was measured using a spectrophotometer.

**Apoptosis detection.** In total,  $1 \times 10^5$  cells were used for the FITC Annexin V Apoptosis detection kit (BD Pharmingen, USA) according to the manufacturer's instructions.

**Western blot.** Antibodies specific for the following proteins were purchased from Cell Signaling and used at a 1:1,000 dilution: AKT, p-AKT, p21, bad, box, bak, caspase 3, caspase 8, caspase 9, cleaved caspase 3, cleaved caspase 8, cleaved caspase 9, p53, p-p53, p-MDM2, PARP and cleaved PARP. The anti-GAPDH antibody was used at a 1:3,000 dilution (Cell Signaling). The anti-MDM2 antibody was purchased from Santa Cruz and used at a 1:500 dilution. The secondary antibody was provided by Earthox (Cat: E030120-01) and used at a 1:3,000 dilution. Western blots were performed according to the protocol provided by Cell Signaling Technology.

**siRNA and small molecule inhibitors.** siRNA oligos were synthesized by JiMA Biotechnological, Inc. (Shanghai, China). siRNA transfections were performed using Lipofectamine 2000 (Invitrogen) according to the manufacturer's protocol. The following siRNA sequences were used: TP53-siRNA-F: 5'-CUACUCCUGAA-AACAACGdTdT-3' and TP53-siRNA-R: 5'-dTdTGAUGAAGGACUUUUGU-UGC-3'. Non-targeted CONTROL siRNA (commercial siRNA) was used as a negative control. For each transfection, 20 nM siRNA was used. Cells were treated with 50  $\mu$ M DHM 12 h after transfection, and the gene mRNA levels and protein expression profiles were measured. PFT $\alpha$  is a chemical compound that inhibits p53-dependent apoptosis. For these studies, cells were treated with 10 mM PFT $\alpha$  to inhibit p53 prior to DHM exposure.

**Immunofluorescence.** Cells were plated in IF culture dishes (Nest, China) and treated with DHM. The cells were then fixed in paraformaldehyde (PFA) and permeabilized with 0.01% triton-X 100. Next, the cells were incubated with primary antibodies (1:500 dilution in PBS with 5% BSA) at 4°C overnight. Dylight 649-conjugated secondary antibodies were applied at a dilution of 1:500 at room temperature for 1 h. The specimens were examined using TCP-SP5 laser confocal microscope (Leica, Germany).

**Real-time quantitative RT-PCR.** mRNA was extracted using TRIzol (Invitrogen, US) and reverse-transcribed to cDNA using the PrimeScript<sup>™</sup> RT Reagent kit with the gDNA Eraser kit (Takara, Japan). SYBR<sup>®</sup> Premix Ex Taq<sup>™</sup>TMII (Takara, Japan) was used to perform real-time quantitative PCR according to the manufacturer's instructions.

**Animal and xenotransplantation experiments.** Animal experiments were conducted following the standards and procedures authorized by the Guang Dong Medical College Animal Care and Use Committee. The protocol was approved by the Committee on the Ethics of Animal Experiments of Guangdong Medical College. (Permit Number: SYXK (Guangdong): 2008-0007). Male BALB/c-nu/nu mice (8–10 weeks of age at the beginning of the experiment) were acquired from the Guang Dong

medical experiment animal center. Mice were allowed free access to autoclaved food and water. HepG2 cells were suspended in PBS at a concentration of  $1 \times 10^7$  cells/ml, and 0.2 ml of the suspension was injected subcutaneously into the left flank of each animal. In total, we selected 18 mice with tumor volumes up to 100 mm<sup>3</sup>. The mice were randomly separated into one of the following three groups (n = 6/each group): the control group, the 150 mg/kg DHM group and the 500 mg/kg DHM group. DHM was dissolved in sodium carboxymethylcellulose (CMC-Na) and administered to the mice twice weekly for 21 days. The control group was administered CMC-Na as a vehicle control.

**Immunohistochemical staining of tumor samples.** Tumor samples were obtained and immediately fixed with PFA. After normal processing, the samples were embedded in paraffin and sliced. The p53 antibody was used at a dilution of 1:500, and the p-p53 antibody was used at a dilution of 1:200. The staining was imaged and analyzed using the Leica pathological analysis software.

**Statistical analysis.** Statistical analysis was performed using the SPSS16.0 software. All data are presented as the mean  $\pm$  SD; error bars represent the SD in all figures. Intergroup comparisons were performed using a two-tailed Student's t-test. A P value < 0.05 was considered statistically significant. \* P < 0.05; \*\* P < 0.01; \*\*\* P < 0.001.

- Feng, M. *et al.* Therapeutically targeting glypican-3 via a conformation-specific single-domain antibody in hepatocellular carcinoma. *P Natl Acad Sci USA* **110**, E1083–E1091 (2013).
- Wilson, T. R. *et al.* Widespread potential for growth-factor-driven resistance to anticancer kinase inhibitors. *Nature* **487**, 505–509 (2012).
- Meyskens, F. L. & Gerner, E. W. Development of Difluoromethylornithine (DFMO) as a Chemoprevention Agent. *Clin Cancer Res* **5**, 945–951 (1999).
- Suzuki, R. *et al.* Effective anti-tumor activity of oxaliplatin encapsulated in transferrin-PEG-liposome. *Int J Pharm* **346**, 143–150 (2008).
- Florea, A.-M. & Büsselberg, D. Cisplatin as an anti-tumor drug: cellular mechanisms of activity, drug resistance and induced side effects. *Cancers* **3**, 1351–1371 (2011).
- Xu, W., Towers, A., Li, P. & COLLET, J. P. Traditional Chinese medicine in cancer care: perspectives and experiences of patients and professionals in China. *Euro J Cancer Care* **15**, 397–403 (2006).
- Zhang, X. W. *et al.* Arsenic trioxide controls the fate of the PML-RARalpha oncoprotein by directly binding PML. *Science* **328**, 240–243 (2010).
- Amin, A. R., Kucuk, O., Khuri, F. R. & Shin, D. M. Perspectives for cancer prevention with natural compounds. *J Clin Oncol* **27**, 2712–2725 (2009).
- Gullett, N. P. *et al.* Cancer prevention with natural compounds. *Semin Oncol* **37**, 258–281 (2010).
- Tsuda, H. *et al.* Cancer prevention by natural compounds. *Drug Metab Pharmacol* **19**, 245–263 (2004).
- Nazemiyeh, H. *et al.* Antioxidant phenolic compounds from the leaves of Erica arborea (Ericaceae). *Nat Prod Res* **22**, (2008).
- Shen, Y. *et al.* Dihydropyridinone as a novel anti-alcohol intoxication medication. *J Neurosci* **32**, 390–401 (2012).
- Shukla, Y. & Singh, M. Cancer preventive properties of ginger: a brief review. *Food Chem Toxicol* **45**, 683–690 (2007).
- Wu, S. *et al.* Dihydropyridinone Reduced Bcl-2 Expression via p53 in Human Hepatoma HepG2 Cells. *PLoS One* **8**, e76886 (2013).
- Vara, J. Á. F. *et al.* PI3K/Akt signalling pathway and cancer. *Cancer Treat Rev* **30**, 193–204 (2004).
- Cardone, M. H. *et al.* Regulation of cell death protease caspase-9 by phosphorylation. *Science* **282**, 1318–1321 (1998).
- Li, W., Zheng, H., Bukuru, J. & De Kimpe, N. Natural medicines used in the traditional Chinese medical system for therapy of diabetes mellitus. *J Ethnopharmacol* **92**, 1–21 (2004).
- Langmead, L. & Rampton, D. Review article: herbal treatment in gastrointestinal and liver disease—benefits and dangers. *Aliment Pharm Therap* **15**, 1239–1252 (2001).
- Ji, H.-F., Li, X.-J. & Zhang, H.-Y. Natural products and drug discovery. *EMBO Rep* **10**, 194–200 (2009).
- Vara, J. Á. F. *et al.* PI3K/Akt signalling pathway and cancer. *Cancer Treat Rev* **30**, 193–204 (2004).
- Hennessy, B. T., Smith, D. L., Ram, P. T., Lu, Y. & Mills, G. B. Exploiting the PI3K/AKT pathway for cancer drug discovery. *Nat Rev Drug Discov* **4**, 988–1004 (2005).
- del Peso, L., Gonzalez-Garcia, M., Page, C., Herrera, R. & Nunez, G. Interleukin-3-induced phosphorylation of BAD through the protein kinase Akt. *Science* **278**, 687–689 (1997).
- Bailey, S. M. *et al.* DNA double-strand break repair proteins are required to cap the ends of mammalian chromosomes. *P Natl Acad Sci USA* **96**, 14899–14904 (1999).
- Rubbi, C. P. & Milner, J. p53 is a chromatin accessibility factor for nucleotide excision repair of DNA damage. *EMBO J* **22**, 975–986 (2003).
- Michael, D. & Oren, M. The p53-Mdm2 module and the ubiquitin system. *Semin Cancer Biol* **13**, 49–58 (2003).
- Moll, U. M. & Petrenko, O. The MDM2-p53 interaction. *Mol Cancer Res* **1**, 1001–1008 (2003).



27. Banin, S. *et al.* Enhanced phosphorylation of p53 by ATM in response to DNA damage. *Science* **281**, 1674–1677 (1998).

## Acknowledgments

The authors thank Dr. Du Feng (Department of Neurology, Affiliated Hospital of Guan Dong Medical College) and Dr. Hege Chen (Department of Urology, Affiliated Hospital of Guan Dong Medical College) for their critical comments. This work was supported in part by the following grants: The National Natural Science Funds (81041099) and Guangdong Province Natural Science Funds (S2011010003750) of China.

## Author contributions

M.L. and R.Z. conceived and directed the project. Q.Z., R.Z. and Y.C. designed the experiments. Q.Z., J.L., B.L., J.X., C.Z., N.C., X.C. and C.L. carried out the experiments. Q.Z. and J.L. conducted the data analysis and interpreted the results. Q.Z. and R.Z. wrote and edited the paper. All authors reviewed the manuscript.

## Additional information

**Supplementary information** accompanies this paper at <http://www.nature.com/scientificreports>

**Competing financial interests:** The authors declare no competing financial interests.

**How to cite this article:** Zhang, Q.Y. *et al.* Dihydromyricetin promotes hepatocellular carcinoma regression via a p53 activation-dependent mechanism. *Sci. Rep.* **4**, 4628; DOI:10.1038/srep04628 (2014).



This work is licensed under a Creative Commons Attribution-NonCommercial-NoDerivs 3.0 Unported License. The images in this article are included in the article's Creative Commons license, unless indicated otherwise in the image credit; if the image is not included under the Creative Commons license, users will need to obtain permission from the license holder in order to reproduce the image. To view a copy of this license, visit <http://creativecommons.org/licenses/by-nc-nd/3.0/>